

## Magnesium removal from an aluminum molten alloy using enriched mineral silica with amorphous nanoparticles of SiO<sub>2</sub>

R.C.B.Tavitas-López<sup>1</sup>, H.M.Hdz-García<sup>1</sup>, R.Muñoz-Arroyo<sup>1\*</sup>, J.C.Escobedo-Bocardo<sup>2</sup>, P.D.Pérez-Coronado<sup>1</sup>, E.E.Granda-Gutierrez<sup>1</sup>

<sup>1</sup>COMIMSA-Salttillo, Ciencia y Tecnología No. 790, Col. Saltillo 400, 25290 Saltillo, Coah., México.

<sup>2</sup>CINVESTAV Unidad Saltillo, Av. Industria Metalúrgica 1062, Parque Industrial Saltillo-Ramos Arizpe, 25900 Ramos Arizpe, Coah., México.

E-mail: rocio.tavitas@comimsa.com, hmanuelhdz@comimsa.com, rita.munoz@comimsa.com, jose.escobedo@cinvestav.edu.mx, patricia.perez@comimsa.com, egranda@comimsa.com

### ABSTRACT

In order to improve the Mg removal from an A-380 molten alloy, mixtures of mineral silica and amorphous silica nanoparticles (SiO<sub>2(NP's)</sub>) were tested. Mineral silica was enriched with 2.5, 5 and 10wt% of amorphous SiO<sub>2(NP's)</sub>. Before Mg removing, samples of mineral silica were impregnated with SiO<sub>2(NP's)</sub> by mixed for 30 min in ethanol and then dried at 110°C for 24 h. The enriched mineral silica with nanoparticles was analyzed by scanning electron microscopy and transmission electron microscopy. The Mg removal was carried out injecting each mixture into the molten aluminum alloy at 750°C using argon as a carrier gas. The Mg content of the molten alloy was measured after different periods of injection time (each 10 min). It was found that the mineral silica with 10wt% of SiO<sub>2(NP's)</sub> is the most efficient mixture, removing Mg from an initial content of 1.6 to a final content of 0.4wt%, in 70 min of injection. Moreover, thermodynamic predictions were carried out in the FactSage software in order to establish chemical equations occurring in the system.

© 2015 Trade Science Inc. - INDIA

### KEYWORDS

Aluminum alloys;  
Magnesium removal;  
Mineral silica;  
Nanoparticles.

### INTRODUCTION

Aluminum is widely used in the manufacture and development of new products due to their excellent physical and chemical properties, mainly low density and high corrosion resistance<sup>[1]</sup>. So, it can be used in automotive and aerospace components. For this reason, the manufacture of aluminum alloys is basically focused in the increasing of the mechani-

cal properties which is a prerequisite for the components that are subject to high stress. In this case, the Al-Si alloy has as mainly alloying elements Fe, Sb, Zn, Mn and Mg<sup>[2]</sup>. It is noticeable that a high content of Mg promotes the growth of the undesirable  $\beta$ -AlFeSi<sup>[3, 4]</sup>.

Therefore, in aluminum foundries a variety of methods to Mg removal are used. The most usual method to remove Mg is chlorination<sup>[5]</sup>. Reports in

## Full Paper

the literature<sup>[5,6]</sup> indicate that it is an efficient method to remove Mg. Nevertheless, this requires a strict control of storage and handling of chlorine gas as well as systems of filtration of gases in order to reduce contaminants. Other authors<sup>[2]</sup> report the use of reactive powders such as  $\text{AlF}_3$ ,  $\text{MgCl}_2$ ,  $\text{KMgCl}_3$ ,  $\text{NaAlF}_4$  in order to remove Mg. These powders can clean and degasify the molten alloy. Besides, the kinetics of Mg removal is very slow and the treatment requires very long times. On the other hand, the electrochemical process is another method that is used in the Mg removal<sup>[7]</sup> and it is considered as a green-process. However, it is necessary to consider that the cost of electricity in some countries is very high.

In this way, the aim of this work was the study of the Mg removal from a A-332 molten aluminum alloy by using mixtures of mineral silica and  $\text{SiO}_{2(\text{NP's})}$  as Mg remover agents. The capacity of these Mg remover agents was evaluated by comparing their effect with that corresponding to the mineral silica.

### EXPERIMENTAL PROCEDURE

#### Raw materials: characterization of mineral silica and $\text{SiO}_{2(\text{NP's})}$

The mineral silica was classified obtaining powders with an average particle size smaller than  $150\ \mu\text{m}$ . The chemical composition of the mineral was determined by atomic absorption spectroscopy, inductively coupled plasma atomic emission spectroscopy, and gravimetric method. Amorphous  $\text{SiO}_{2(\text{NP's})}$  (Aldrich, 99.99%) with size smaller than 10 nm were selected for this work. These nanoparticles were characterized by TEM.

#### Impregnation and characterization of mineral silica with amorphous $\text{SiO}_{2(\text{NP's})}$

The impregnation of mineral silica with amorphous  $\text{SiO}_{2(\text{NP's})}$  were reached mixing the selected amount of nanoparticles (2.5, 5 and 10wt%) with mineral silica for 30 min in ethanol and drying the mixture in a furnace at 110 °C for 24 h. Samples of the enriched mineral silica were analyzed by SEM.

#### Thermodynamic predictions

Using the Gibbs free energy minimization algorithm implemented in the Equilib module of the FactSage package was considered in order to obtain thermodynamics predictions using the stoichiometry of reaction (1) and real experimental data. Likewise, in order to establish the reaction products as a function of increasing of  $\text{SiO}_{2(\text{NP's})}$  impregnated in the mineral silica (2.5, 5 and 10%).

#### Experimental procedure for the Mg removal tests

The selected alloy was the 332 aluminum base alloy (TABLE 2). An induction electric furnace, equipped with a silicon carbide crucible and temperature control, was used to melt and hold the alloy. Injection equipment, with devices to measure and control the gas and powder flows, was used to introduce the powder mixtures into the melt. The injection lance, with an internal diameter of 6.98 mm, was made of graphite. The selected parameters for the submerged powder injection experiments were argon (99.9999%) flow of 4 L Ar/min, powder flow of 16 g/min, mass of aluminum alloy of 6 kg, and aluminum alloy treatment temperature of 750 °C. The lance was submerged at the 85% of the depth of the melt. The variable in the experiments was the composition of the powder mixtures mineral- $\text{SiO}_{2(\text{NP's})}$  to be injected (0.0, 2.5, 5 and 10% of  $\text{SiO}_{2(\text{NP's})}$ ). The mass of the powders to be injected was calculated considering the  $\text{SiO}_2$  as the solid reagent and

TABLE 1 : Chemical composition of mineral silica obtained by atomic absorption

Mineral	K (wt-%)	Ca (wt-%)	Na (wt-%)	$\text{SiO}_2$ (wt-%)	Fe (wt-%)	Mg (wt-%)	Mn (wt-%)	$\text{CO}_3$ (wt-%)	Al (wt-%)
Silica	0.004	0.059	0.022	99.19	0.080	0.010	<0.001	0.070	0.155

TABLE 2 : Chemical composition of the A-332 alloy, obtained by inductively coupled plasma atomic emission spectroscopy

Si (wt-%)	Fe (wt-%)	Mn (wt-%)	Mg (wt-%)	Cu (wt-%)	Zn (wt-%)	Ti (wt-%)	Cr (wt-%)	Ni (wt-%)	Al (wt-%)
8.060	0.517	0.341	1.600	3.410	0.398	0.128	0.029	0.032	85.484

spinel and silicon as products according to the chemical reaction (1).



For each experiment, samples of the melt were obtained every 10 min and the produced dross (oxidized material) was collected at the end of the experiment. The solidified samples were analyzed by spark atomic emission spectrometry to determine their chemical compositions and a sample of the dross was analyzed by XRD. Additionally, the quantity of slag was weighted and the efficiency of process was calculated (Eq.2).

Efficiency:

$$\eta = \frac{\% \text{Mg}_i - \% \text{Mg}_f}{\% \text{Mg}_i} \quad (2)$$

Where;  $\% \text{Mg}_i$  is the initial percent of magnesium and  $\% \text{Mg}_f$  is the final percent of magnesium.

Thermodynamic predictions about the studied system were carried out using the FactSage software.

### Characterization of reaction products

In order to determine the reaction products, samples of the slags formed during the injection tests were characterized by X-ray diffraction (XRD).

## RESULTS AND DISCUSSION

### Raw materials characterization

TABLE 1 shows the chemical composition, obtained by atomic absorption, of mineral silica. As can be seen, silica is 99.19wt% pure and the others

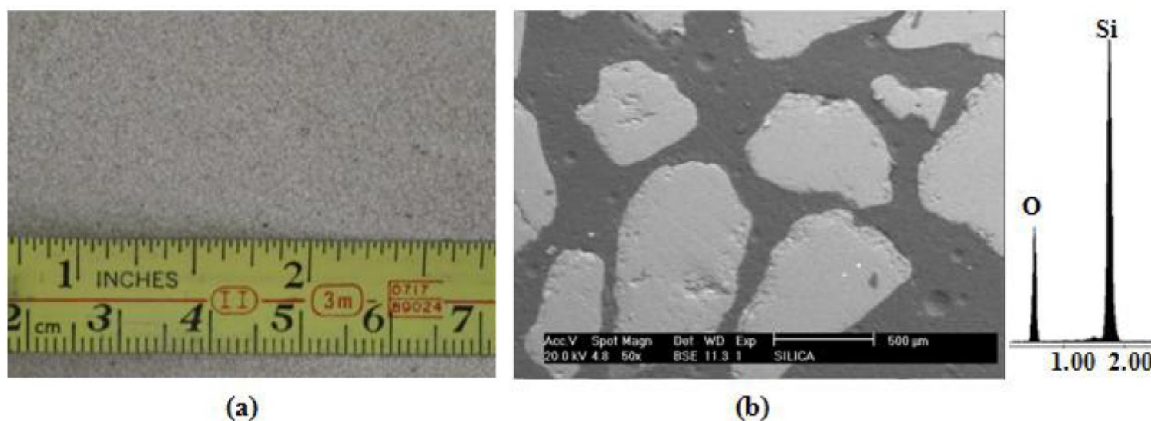


Figure 1 : Mineral silica: (a) as received and (b) SEM image of mineral silica without nanoparticles of amorphous  $\text{SiO}_2(\text{NP's})$

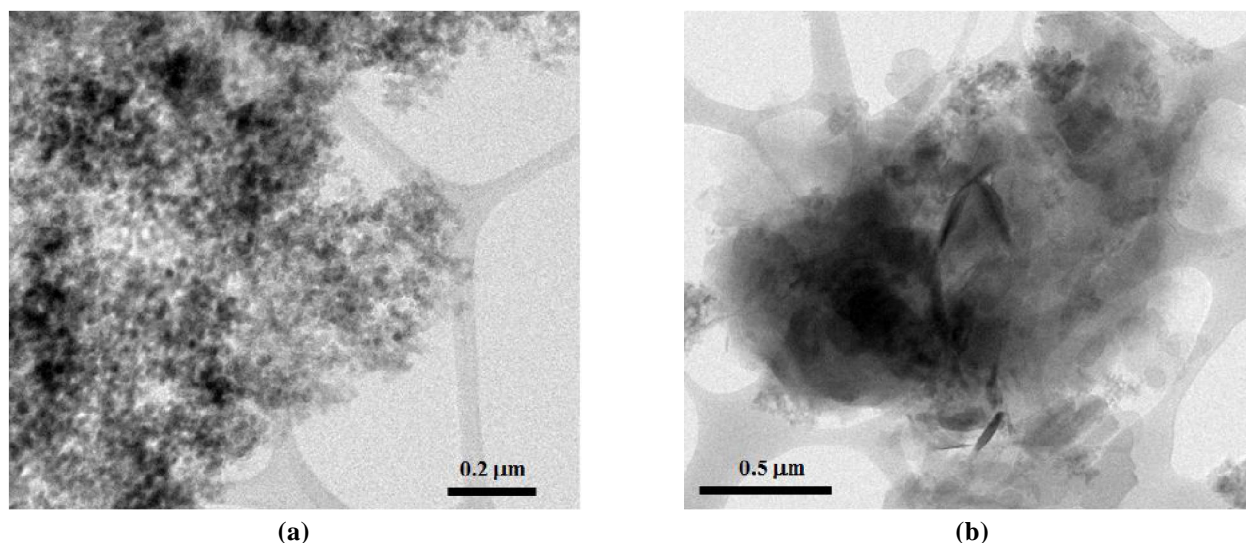


Figure 2 : TEM images: (a) amorphous  $\text{SiO}_2$  nanoparticles as received and (b) impregnated mineral silica with 10wt% of  $\text{SiO}_2(\text{NP's})$

## Full Paper

elements do not influence in the Mg removal process. Reports in the literature<sup>[8, 9]</sup> suggest that silica can remove the Mg of molten alloys using the injection method of enriched-silica powders when the initial Mg content is 1.0wt%<sup>[9]</sup>. Additionally, TABLE 2 shows the chemical composition, obtained by inductively coupled plasma atomic emission spectroscopy, of the A-332 molten aluminum alloy.

Figure 1(a) shows the mineral silica as received. Figure 1(b) presents a SEM image of particles of this material (regular morphology) and the corresponding EDX which indicates that the particles are composed of silicon and oxygen.

### Characterization of the enriched mineral silica with amorphous SiO<sub>2(NP's)</sub>

Amorphous SiO<sub>2(NP's)</sub> nanoparticles as received and a sample of mineral silica with 10wt% of SiO<sub>2(NP's)</sub> were analyzed by TEM (Fig. 2 (a) and (b)). At high amplification, it is observed that the SiO<sub>2(NP's)</sub> have a spherical morphology as received (Figure

2(a)). The enriched mineral silica with 10wt% of SiO<sub>2(NP's)</sub> shows nanoparticles agglomerates at different zones (Figure 2(b)). This surface aspect can affect the rate and time of Mg removal due to that increase the surface energy by the nanoparticle sizes, increasing the reaction kinetics.

### Thermodynamic predictions and selection of the al alloy and Mg removal by injection

In regards to Eq. 1, the feasibility of this reaction was determined thermodynamically in the Equilib module of FactSage. Based in this equation and considering the amount of Mg in the alloy, the mass balances for the mineral silica without and with SiO<sub>2(NP's)</sub> were performed. As can be seen in the Fig. 3, at least the formation of spinel and Si are predicted in accordance with Eq. 1, as proposed in literature [8].

Therefore, as a preliminary step to the removal process of Mg were carried on thermodynamic predictions simultaneously with real experimental data

Page 1 - 750 C  
(gram) Mg + 2 Al + 2 SiO2 =

+	1.2059	gram	Spinel	
			( 750.00 C, 1.0000 atm)	
			15.366	wt.% Al3O4[1+]
			0.58663E-10	wt.% Al104[5-]
			76.701	wt.% Mg1Al2O4
			1.3248	wt.% Al1Mg2O4[1-]
			6.6080	wt.% Mg3O4[2-]
			0.28955E-09	wt.% Mg1O4[6-]
+	1.3166	gram	Monoxide	
			( 750.00 C, 1.0000 atm)	
			100.00	wt.% MgO
			0.21077E-24	wt.% Al2O3
+			1.5426	gram Al_liquid
			( 750.00 C, 1.0000 atm, liq, a= 1.0000 )	
+			0.93487	gram Si_solid
			( 750.00 C, 1.0000 atm, s, a= 1.0000 )	
H				G
(J)				(J)
			-3.46637E+04	
				-4.58233E+04

Figure 3 : Thermodynamic predictions calculated in the equilib module of FactSage

TABLE 3 : Amounts of reactants considered for Mg removal, calculated at 750 with 21 g of O<sub>2</sub> using the Equilib and Reaction modules of FactSage

Reactions	Al (kg)	Mg (kg)	SiO <sub>2</sub> (kg)
1) Silica+2.5%SiO <sub>2(NP's)</sub>	6.00	0.096	0.0963
2) Silica+5%SiO <sub>2(NP's)</sub>	6.00	0.096	0.01925
3) Silica+10%SiO <sub>2(NP's)</sub>	6.00	0.096	0.03850

in the FactSage package as follows: 1) First, a series of calculations were made in the Equilib module in order to obtain the Gibbs free energy minimization and 2) in the Reaction module was illustrated the graph of free energy of the reactions varying the content in g of  $\text{SiO}_{2(\text{NPs})}$  at  $750^\circ\text{C}$ , 1 atm and considering 21 g of  $\text{O}_2$  (TABLE 3).

As can be seen in the Figure 4, the Gibbs free energies are more spontaneous when the content of

$\text{SiO}_2$  is increased according to the labeled reactions in the TABLE 3.

### Experimental procedure for the Mg removal tests

Figure 5 shows the variation of the Mg content in the aluminum alloy as a function of the injection time for the different experiments. As it can be observed in Figure 5, when mineral silica is used Mg is removed from its initial concentration (1.6wt %)

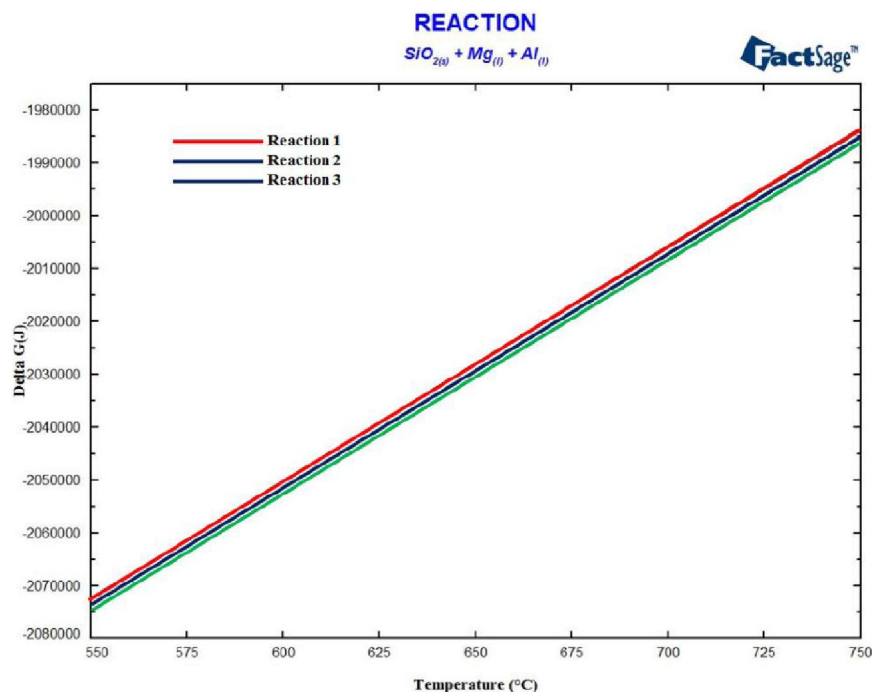


Figure 4 : Diagram of gibbs free energy for Mg removal calculated in FactSage

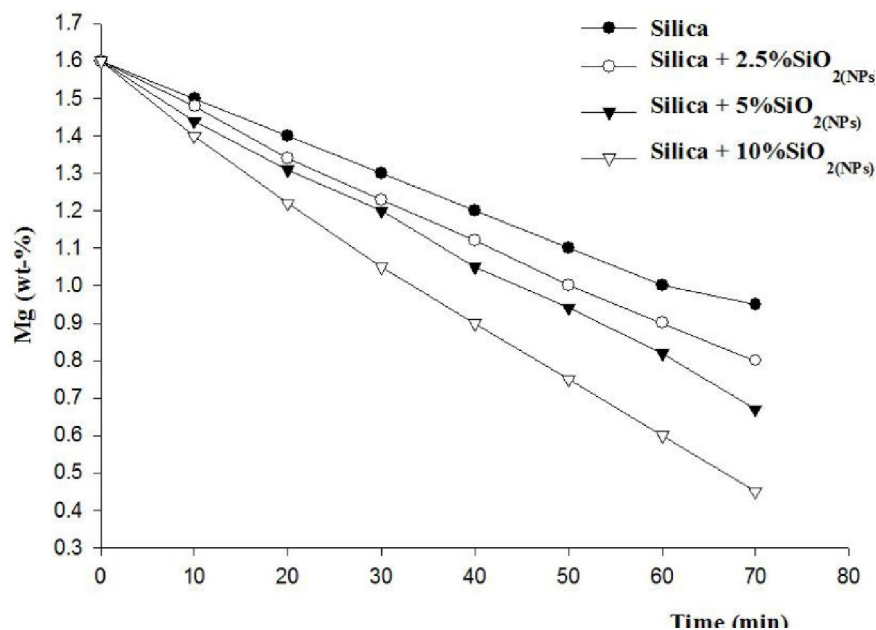


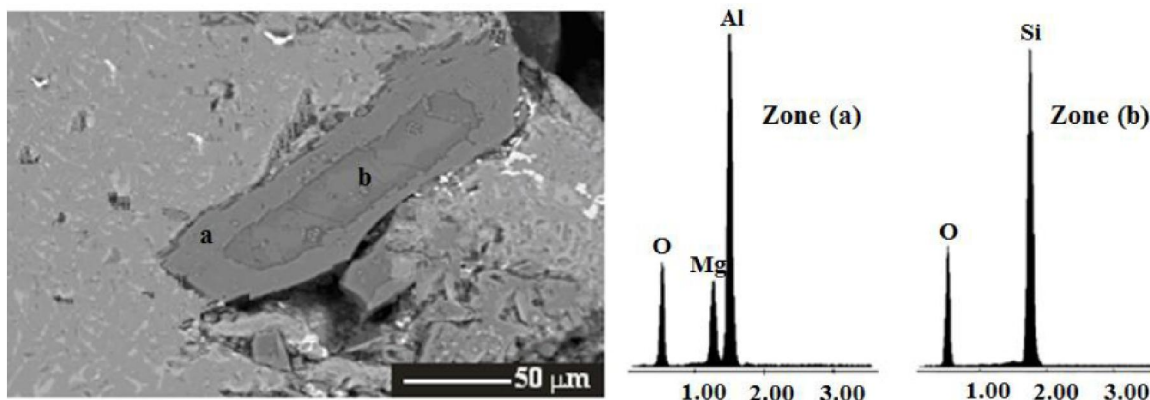
Figure 5 : Mg content in the alloy as a function of the injection time for the performed experiments

TABLE 4 : Amounts of reactants considered for Mg removal

Samples	W <sub>initial ingot</sub> (kg)	W <sub>final ingot</sub> (kg)	W <sub>slag</sub> (kg)	%Mg		η (%)
				initial	final	
SiO <sub>2</sub>	6	3.800	1.240	1.6	0.94	41.250
SiO <sub>2</sub> + 2.5%SiO <sub>2(NPS)</sub>	6	2.600	0.863	1.6	0.81	49.375
SiO <sub>2</sub> + 5%SiO <sub>2(NPS)</sub>	6	2.904	0.549	1.6	0.67	58.125
SiO <sub>2</sub> + 10%SiO <sub>2(NPS)</sub>	6	2.904	0.498	1.6	0.44	72.500

TABLE 5 : Main reaction products identified in the slag using XRD analysis

Compound	Silica	Silica+ 2.5%SiO <sub>2(NPS)</sub>	Silica+ 5%SiO <sub>2(NPS)</sub>	Silica+ 10%SiO <sub>2(NPS)</sub>
Al	X	X	X	X
Si	X	X	X	X
SiO <sub>2</sub> quartz	X	X	X	X
MgO periclase	X	X	X	X
MgAl <sub>2</sub> O <sub>4</sub> spinel	X	X	X	X
Mg <sub>2</sub> (SiO <sub>4</sub> ) forsterite		X	X	X
Al <sub>2</sub> O <sub>3</sub> corundum	X			

Figure 6 : SEM image of a semi-reacted silica particle and corresponding EDX: a) shell of spinel and b) SiO<sub>2</sub> unreacted center

to a final concentration of 0.95wt%. By contrast, the best results were obtained when a mixture containing 10% of SiO<sub>2(NPS)</sub> was used, reaching a final Mg concentration of 0.48wt%. This behavior can be explained considering that the increase of the surface energy due to the silica nanoparticles and the stirring conditions into the molten alloy created by the magnetic induction forces of the furnace and the carrier gas flow, contribute to the Mg removal. The amount of Mg removed from the molten alloy was a direct function of the amount of nanoparticles in the mixture mineral silica-SiO<sub>2(NPS)</sub>.

TABLE 4 shows the Mg removal efficiency (η) for each experiment. It is noticeable that the efficiency increases in the mixtures of mineral silica with 5 and 10wt% of SiO<sub>2(NPS)</sub> due to the surface

energy of the mineral silica is modified by the impregnated nanoparticles, this fact increases the kinetics of Mg removal. On the other hand, it was further observed that by using mixtures of mineral silica and nanoparticles, a smaller amount of slag was generated. In addition, stable oxides such as MgAl<sub>2</sub>O<sub>4</sub>(spinel), MgO(periclase) and Mg<sub>2</sub>SiO<sub>4</sub>(forsterite) as well as SiO<sub>2</sub>(quartz) are formed and they were identified in the slag by XRD as can be seen in the TABLE 5.

It has been postulated that the decrease in the Mg removal rate is due to the formation of a spinel shell on the surface of the mineral silica particle, shell that continuously grows. According to the chemical reaction (1), spinel is a final product with high thermodynamic stability. A semi-reacted silica

particle is observed in Figure 6, showing a shell of spinel on the surface of an unreacted mineral silica nucleus.

## CONCLUSIONS

Mineral silica enriched with 10wt% of  $\text{SiO}_{2(\text{NP's})}$  demonstrated its capacity as Mg remover. The Mg removal rate from the molten alloy is reduced due to the formation of a spinel shell on the surface of the silica particles. It is noticeable that the use of this mineral silica with  $\text{SiO}_2$  nanoparticles reduces the amount of generated slag, decreasing the metal losses by oxidation. In addition, it was found that the Gibbs free energy minimization algorithm for the Mg removal can be predicted through the combination of Equilib and Reaction modules in order to establish a balance of mass.

## REFERENCES

- [1] F.Samuel, S.Gowri; Effect of Mg on the solidification behavior of two Al-Si-Cu-Fe-Mg (380) diecasting alloys, *Transactions of the American*, **101**, 611-618 (1993).
- [2] G.Gaustad, E.Olivetti, R.Kirchain; Improving aluminum recycling: A survey of sorting and impurity removal technologies, *Resources, Conservation and Recycling*, **58**, 79-87 (2012).
- [3] S.Gowri, F.Samuel; Effect of alloying elements on the solidification characteristics and microstructure of Al-Si-Cu-Mg-Fe 380 Alloy, *Metallurgical and materials transactions*, **25A**, 437-448 (1994).
- [4] L.Anantha Narayanan, F.H.Samuel, J.E.Gruzleski; Crystallization behavior of iron-containing intermetallic compounds in 319 aluminum alloy, *Metallurgical and materials transactions*, **25A(8)**, 1761-1773 (1994).
- [5] E.A.Vieira, J.R.De Oliveira, G.F.Alves, D.C.R.Espinosa, J.A.S.Tenorio; *Materials Transactions*, **53(3)**, 477-482 (2012).
- [6] V.D.Neff V, P.B.Cochran; Light Metals, U.S.A., Panel for Aluminum Processing, 1053-1060 (1993).
- [7] B.L.Tiwari, B.J.Howie, R.M.Johnson; AFS Transactions, U.S.A., 385-390 (1986).
- [8] R.A.Muñoz, J.C.B.Escobedo, H.M.G.Hdez, D.A.H.Cortés, M.M.Terrones, A.P.Rodríguez, J.L.P.Hernández; *Revista de Metalurgia*, **46(4)**, 1988-4222 (2010).
- [9] F.Carmona-Muñoz, H.M.Hdz-García, R.Muñoz-Arroyo, J.C.Escobedo-Bocardo, D.A.Cortés-Hernández; *Chemical Technology, An Indian Journal*, **8(4)**, 115-120 (2013).